

# Formation Mechanism of Condensation Nuclei in Nighttime Atmosphere and the Kinetics of the SO<sub>2</sub>-O<sub>3</sub>-NO<sub>2</sub> System

Zhilong Diane Xie

Environmental Studies Institute, Drexel University, Philadelphia, Pennsylvania 19104  
(Received: October 18, 1991; In Final Form: December 26, 1991)

An experimental study of condensation nuclei formation for the system of SO<sub>2</sub>-O<sub>3</sub>-NO<sub>2</sub>-water vapor-zero grade air at 1 atm and room temperature has been conducted. In the experiments, nitrogen dioxide and ozone were mixed to generate NO<sub>3</sub> and N<sub>2</sub>O<sub>5</sub>; the O<sub>3</sub>/NO<sub>2</sub>/NO<sub>3</sub>/N<sub>2</sub>O<sub>5</sub> mixture and sulfur dioxide and water vapor were introduced into a specially designed sheath flow reaction vessel in which the oxidation of sulfur dioxide by NO<sub>3</sub> and N<sub>2</sub>O<sub>5</sub> occurred to produce condensation nuclei which were quantitatively determined. The results of several series of experiments accomplished at different concentrations of each of the reactants are presented. The correlations of observed concentrations of condensation nuclei to concentrations of sulfur dioxide, nitrogen dioxide, ozone, and water vapor are evaluated. A model of the mechanism of condensation nuclei formation in nighttime atmosphere is established. From the kinetic analysis of the experimental results, estimates are derived for the rate constants of the following reactions, SO<sub>2</sub> + NO<sub>3</sub> → SO<sub>3</sub> + NO<sub>2</sub>,  $k \leq 4.5 \times 10^{-21}$  cm<sup>3</sup> molecule<sup>-1</sup> s<sup>-1</sup>; and SO<sub>2</sub> + N<sub>2</sub>O<sub>5</sub> → SO<sub>3</sub> + N<sub>2</sub>O<sub>4</sub>,  $k = 9.1 \times 10^{-24}$  cm<sup>3</sup> molecule<sup>-1</sup> s<sup>-1</sup>, at 26.5 °C, which are below the upper limit values reported previously.

## Introduction

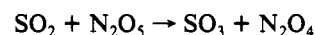
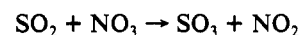
A major atmospheric environmental problem in many parts of the world is caused by sulfur dioxide. The concentration of SO<sub>2</sub> is significantly elevated by anthropogenic sources such as the combustion of sulfur-containing fossil fuel. The homogeneous oxidation of SO<sub>2</sub> makes small condensation nuclei in gas-to-particle conversion. These are the new particles in the atmosphere. The principle environmental problem associated with condensation nuclei formation is visibility degradation in arid regions.

In order to understand how sulfate aerosols are formed, it is important to investigate the formation mechanism of condensation nuclei of sulfuric acid and it is also important to evaluate the rate constants of the gas-phase reactions.

Cadle et al.<sup>36</sup> reported that samples collected in the stratosphere indicate the presence of sulfuric acid aerosols with diameters below 0.1 μm. Sulfuric acid molecules in the presence of water vapor can behave as nucleating agents in the atmosphere to form Aitken nuclei or condensation nuclei which in turn grow to form aerosol particles. Heteromolecular homogeneous condensation nucleation theory is a thermodynamic explanation of the association of gas molecules in a two-component system in which no nucleating surfaces are available. In particular, the system of interest is that of sulfuric acid and water vapor. Scientific reports concerning the processes of nucleation in two-component systems have appeared in the literature.<sup>37-45</sup>

There are a number of candidate reactions<sup>1</sup> for the oxidation of ground-state SO<sub>2</sub>. However, all available evidence suggests that a fast and efficient reaction for sulfuric acid nuclei formation by gas-phase processes is oxidation of SO<sub>2</sub> with the OH radical<sup>2-13</sup> which is a secondary product of ozone photolysis. The formation

mechanism of sulfuric acid nuclei at nighttime has remained unknown. A study by Bandy, Thornton, and co-workers<sup>14,17</sup> in the Arctic atmosphere showed unusually high apparent condensation nuclei production rates in April which could not be reasonably attributed to OH reaction with SO<sub>2</sub> only. One of the possible explanations for these unusual rates is the reaction of SO<sub>2</sub> with NO<sub>3</sub> and/or N<sub>2</sub>O<sub>5</sub>. However, nucleation in the system of SO<sub>2</sub>-NO<sub>2</sub>-O<sub>3</sub>-water vapor at nighttime in a polluted atmosphere has not been systematically explored. Even though some researchers have investigated the oxidation of SO<sub>2</sub> by NO<sub>3</sub> and N<sub>2</sub>O<sub>5</sub>,<sup>15,16,18-20</sup> the reaction rate constants for the following reactions have remained uncertain.



The sulfur trioxide formed from the above reactions would react rapidly with water vapor to produce H<sub>2</sub>SO<sub>4</sub> through the following reaction: SO<sub>3</sub> + H<sub>2</sub>O → H<sub>2</sub>SO<sub>4</sub>. Although numerous papers<sup>46-49</sup>

- (1) Finlayson-Pitts, B. J.; Pitts, Jr., J. N., *Atmospheric Chemistry: Fundamental and Experimental Techniques*; John Wiley & Sons: 1986; p 649.
- (2) Benson, S. W. *Chem. Rev.* **1978**, *78*, 23.
- (3) Stockwell, W. R.; Calvert, J. G. *Atmos. Environ.* **1983**, *17*, 2231.
- (4) Marigitan, J. J. *J. Phys. Chem.* **1984**, *88*, 3314.
- (5) Leu, M. T. *J. Phys. Chem.* **1982**, *86*, 4558.
- (6) Wine, P. H.; Thompson, R. J.; Ravishankara, A. R.; Semmes, D. H.; Gump, C. A.; Torabi, A.; Nicovich, J. M. *J. Phys. Chem.* **1984**, *88*, 2095.
- (7) Cox, R. A. *Int. J. Chem. Kinet. Symp.* **1975**, *1*, 379.
- (8) Davis, D. D.; Ravishankara, A. R.; Fischer, S. *Geophys. Res. Lett.* **1979**, *6*, 113.
- (9) Atkinson, R.; Perry, R. A.; Pitts, J. N. *J. Chem. Phys.* **1976**, *65*, 306.
- (10) Castleman, A. W.; Tang, I. N. *J. Photochem.* **1977**, *6*, 349.
- (11) Harris, G. W.; Atkinson, R.; Pitts, J. N. *Chem. Phys. Lett.* **1980**, *69*, 378.
- (12) Burrows, J. P.; Tyndall, G. S.; Moortgat, G. K. *Chem. Phys. Lett.* **1985**, *119*, 193.
- (13) Cox, R. A.; Shepperd, D. *Nature (London)* **1980**, *284*, 330.

- (14) Thornton, D. C.; Bandy, A. R.; Drieder III, A. R. Sulfur Dioxide in the North American Arctic. In press.
- (15) Daubendiek, R. L.; Calvert, J. G. *Environ. Lett.* **1975**, *8*, 103-116.
- (16) Peter, W. *Chemistry of the Natural Atmosphere*; Academic Press: New York, 1988; p 731.
- (17) Bandy, A. R. Atmospheric Arctic Chemistry. Proposal to the National Science Foundation, 1988, p 8, and personal discussion with A. R. Bandy and his co-workers.
- (18) Burrows, J. P.; Tyndall, G. S.; Moortgat, G. K. *J. Phys. Chem.* **1985**, *89*, 4848-4856.
- (19) Wallington, T. J.; Cox, R. A. *J. Chem. Soc., Faraday Trans.*, **2** **1986**, *82*, 275-289.
- (20) Wallington, T. J.; Atkinson, R.; Winer, A. M.; Pitts, Jr., J. N. *J. Phys. Chem.* **1986**, *90*, 5393-5396.
- (21) Davis, D. D.; Klauber, G. *Int. J. Chem. Kinet. Symp.* **1975**, *1*, 543-556.
- (22) Nolan, P. M. Condensation Nuclei Formation by Photo-oxidation of Sulfur Dioxide with OH Radical in the Presence of Water Vapor and Ammonia. Doctoral Dissertation, Drexel, 1987.
- (23) Demore, W. B.; Molina, M. J.; Watson, R. T.; Golden, D. M.; Hampson, R. F.; Kurylo, M. J.; Howard, C. J.; Ravishankara, A. R. "Chemical Kinetics and Photochemical Data for Use in Stratospheric Modeling". Evaluation No. 6; JPL Publication 83-86, September 15, 1983.
- (24) Finlayson-Pitts, B. J.; Pitts, Jr., J. N. *Atmospheric Chemistry: Fundamental and Experimental Techniques*; John Wiley & Sons: New York, 1986.
- (25) Graham, R. A.; Johnston, H. S. *J. Phys. Chem.* **1978**, *82*, 254.
- (26) Atkinson, R.; Lloyd, A. C. *J. Phys. Chem. Ref. Data* **1984**, *13*, 315.
- (27) Borell, P.; Cobos, C. J.; Croce de Cobos, A. E.; Hippler, H.; Luther, K.; Ravishankara, A. R.; Troe, J.; *Ber. Bunsenges. Phys. Chem.* **1985**, *89*, 337.
- (28) Smith, C. A.; Ravishankara, A. R.; Wine, P. H. *J. Phys. Chem.* **1985**, *89*, 1423.

have been published dealing with the rate constant of this reaction, the detailed mechanism of the  $\text{SO}_3$  to nuclei conversion process has not been well established. The kinetics of nuclei formation via this reaction may be considerably more complex than if it were a simple bimolecular reaction as written. However, a rate constant of  $4.0 \times 10^{-5} \text{ s}^{-1}$  for the isomerization of sulfur trioxide hydrate ( $\text{SO}_3 \cdot \text{H}_2\text{O}$ ) to condensation nuclei conversion was obtained by Nolan.<sup>22</sup>

In this Letter we report the first measurement of the concentrations of the condensation nuclei formed from the system of  $\text{SO}_2$ - $\text{NO}_2$ - $\text{O}_3$  in the presence of water vapor. Kinetic analysis of gas-phase reactions has been performed to evaluate the oxidation reactions of rate constants of the  $\text{SO}_2$  by  $\text{NO}_3$  and  $\text{N}_2\text{O}_5$  radicals and the rate of condensation nuclei formation as a function of concentrations of reactants, sulfur dioxide, nitrogen dioxide, ozone, and water vapor. Our study will provide new information on the formation mechanism of condensation nuclei at nighttime atmosphere.

### Experimental Section

The experiment was carried out by using a fast flow reaction system facility. The system consists of five independent connected devices: generation and control of reactants, flow control, reactant mixing, sheath flow reaction vessel, detection of condensation nuclei, and data recorder (Figure 1).

The dilution of the reactant, sulfur dioxide, was performed by mixing a known concentration of sulfur dioxide/nitrogen mixture ( $9.838 \pm 1\%$ ) ppm in ultra-high-purity nitrogen (from Scott Specialty Gases), with zero grade air (from AIRCO Special Gases contains less than 1 ppm of total hydrocarbon impurities) in the glass mixing bulb 2 in Figure 1. The flow rate of the zero grade air was controlled by a rotameter (Model 62-PVB, Matheson) which maintained a total flow rate through the reaction vessel at a flow rate of  $1500 \text{ cm}^3/\text{min}$ . The water vapor concentration was generated and controlled by changing the flow rate of zero air through a hydrated molecular sieve bed saturated by deionized water. The water vapor concentration in the reaction vessel was calibrated using a frost point hygrometer.<sup>22</sup> Nitrogen trioxide and dinitrogen pentoxide radicals were prepared by reacting nitrogen dioxide with ozone. A specially prepared mixture containing 999 ppm of nitrogen dioxide in nitrogen,  $\text{NO}_2/\text{N}_2$ , in a standard AL tank was used (Scott Specialty Gases). The nitrogen dioxide in nitrogen was mixed with ozone and the carrier gas, zero air, in the glass mixing bulb 1. The gas mixture of  $\text{NO}_3$ ,  $\text{N}_2\text{O}_5$ ,

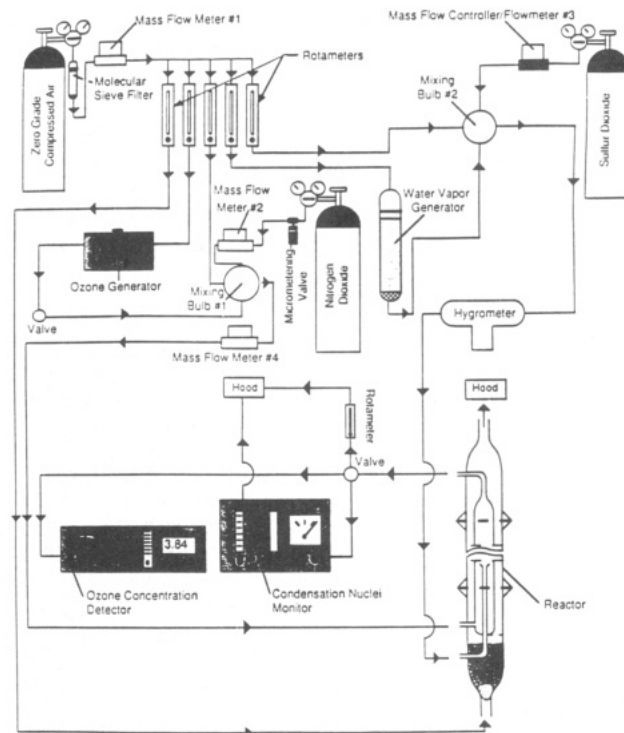


Figure 1. Schematic diagram of experimental flow apparatus.

$\text{NO}_2$ ,  $\text{O}_3$ ,  $\text{N}_2$ , and zero grade air was then introduced into the sheath flow reaction vessel and the flow rate was maintained at a total flow of  $110.0 \text{ cm}^3/\text{min}$  and the flow rate was monitored with a Hasting mass flow meter (Model ST-500X) (mass flow meter, 4 in Figure 1).

The reactants, sulfur dioxide and water vapor, were then mixed and conducted into the reaction vessel. Subsequently, in the reactants flow, the  $\text{NO}_3$  and  $\text{N}_2\text{O}_5$  radicals reacted with the sulfur dioxide molecules to produce sulfur trioxide which further reacted with water vapor to produce condensation nuclei. The condensation nuclei concentration was detected with a condensation nuclei counter (CNC) (Model Rich 100, Environment One Corp.). A series of experiments was performed at different concentrations of the reactants.

The gas reaction and condensation nuclei formation were carried out in a cylindrical Pyrex glass sheath flow reaction vessel which is shown schematically in Figure 2. The reactor was oriented for flow in the vertical direction. A mixture of sulfur dioxide and water vapor was introduced into the reaction vessel through tube A and the gas mixture of  $\text{NO}_3$ ,  $\text{N}_2\text{O}_5$ ,  $\text{NO}_2$ ,  $\text{O}_3$ ,  $\text{N}_2$ , and zero grade air was introduced into the reaction vessel through tube B. Tubes A and B were concentric with the reaction vessel so that sulfur dioxide, water vapor, and  $\text{NO}_3$ ,  $\text{N}_2\text{O}_5$  radicals react at the center of the reaction vessel to produce condensation nuclei. At the same time, the zero air was introduced into the reaction vessel at a constant flow rate of  $1000 \text{ cm}^3/\text{min}$  through tube C. In order to obtain uniform annular sheath flow, 4 mm diameter glass beads were used to fill the bottom portion of the reactor. The uniformity of the annular flow was verified by a test using smoke as a tracer to visualize the flow. The principal advantage of this technique is to minimize diffusion losses of the nuclei and eliminate wall reactions.

The experiment was performed under atmospheric-like conditions where the total air pressure was kept at 1 atm ( $761 \pm 2 \text{ mmHg}$ ), the relative humidity at 1–6%, the reaction temperature was kept at  $26.5 \pm 1 \text{ }^\circ\text{C}$ .

### Results

All of the experiments performed in this study were carried out with continuous flow addition of reactants to the fast flow reaction system. In each experiment, the particle background of the reactant mixture was determined at the same conditions of the

(29) Burrows, J. P.; Tyndall, G. S.; Moortgat, G. K. *Chem. Phys. Lett.* **1985**, *119*, 193.

(30) Burrows, J. P.; Tyndall, G. S.; Moortgat, G. K. *J. Phys. Chem.* **1985**, *89*, 4848.

(31) Tuazon, E. C.; Sanhueza, E.; Atkinson, R.; Carter, W. P. L.; Winer, A. M. *J. Phys. Chem.* **1984**, *88*, 3095–3098.

(32) Huie, R. E.; Herron, J. T. *Chem. Phys. Lett.* **1974**, *27*, 3.

(33) Graham, R. A.; Johnston, H. S. *J. Chem. Phys.* **1974**, *60*, 11.

(34) Webster, C. R.; May, R. D.; Toumi, R.; Pyle, J. A. *J. Geophys. Res.* **1990**, *95*, D9, 13851–13866.

(35) Davidson, J. A.; Cantrell, C. A.; Shetter, R. E.; McDaniel, A. H.; Calvert, J. G. *Geophys. Res.* **1990**, *95*, D9, 13963–13969.

(36) Cadle, R. D.; Lazrus, A. L.; Pollock, W. H.; Shedlovsky, J. P. "The Chemical Composition of Aerosol Particles in the Tropical Stratosphere", CIAP, 1973.

(37) Smith, J. P.; Urone, P. *Environ. Sci. Technol.* **1974**, *8*, 742.

(38) Marvin, D. C.; Reiss, H. *J. Chem. Phys.* **1978**, *69*, 1897.

(39) Flood, H. Z. *Phys. Chem.*, **A** **1934**, *170*, 286.

(40) Mirabel, P.; Clavelin, J. L. *J. Phys. Chem.* **1978**, *68*, 5020.

(41) Mirabel, P.; Katz, J. L. *J. Phys. Chem.* **1974**, *60*, 1138.

(42) Heist, R. H.; Reiss, H. *J. Phys. Chem.* **1974**, *61*, 573.

(43) Shugard, W. J.; Reiss, H. *J. Phys. Chem.* **1976**, *65*, 2827.

(44) Calvert, J. G.; Lazrus, A.; Kok, G. L.; Heikes, B. G.; Walega, J. G.; Lind, J.; Cantrell, C. A. *Nature* **1985**, *317*, 5.

(45) Hamill, P.; Kiang, C. S.; Cadle, R. D. *J. Atmos. Sci.* **1977**, *34*, 150.

(46) Holland, P. M.; Castleman, Jr., A. W. *Chem. Phys. Lett.* **1978**, *56*, 511.

(47) Westberg, K.; Bott, J. F.; Coffey, J.; Durso, S.; Holloway, J. "A Study of the Formation of Sulfuric Acid Aerosols"; Aerospace Corp. Report No. ATR-85 (7899), 1985.

(48) Chen, T. S.; Moore Plummer, P. L. *J. Phys. Chem.* **1985**, *89*, 3689.

(49) Wang, X.; Jin, Y. G.; Suto, M.; Lee, C. *J. Chem. Phys.* **1988**, *89*, 4853.

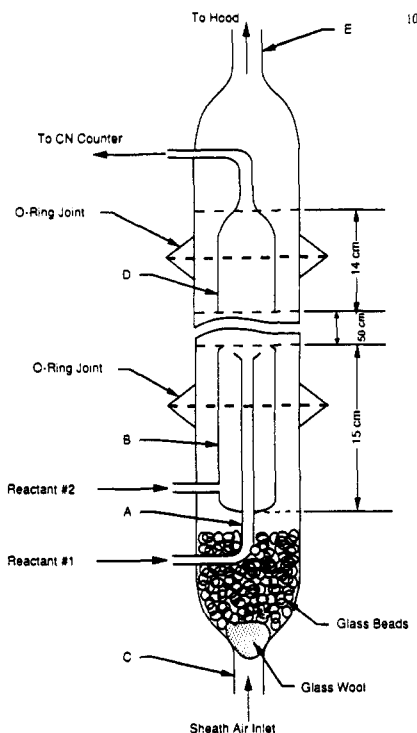


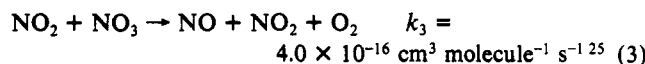
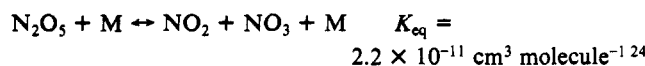
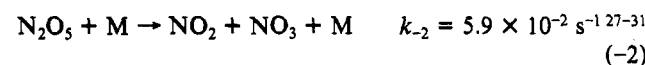
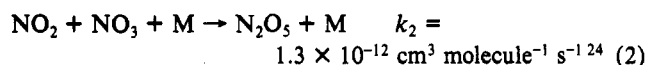
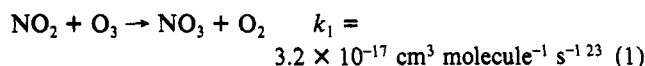
Figure 2. Sheath flow reactor.

experiment except keeping the ozone generator off. The condensation nuclei concentration result was corrected by subtracting the blank value from the CN concentration. There was no observed condensation nuclei concentration when nitrogen dioxide was absent from the reactant mixture.

The experimental data were collected with varied  $\text{SO}_2$  concentrations in the reaction vessel from  $6.56 \times 10^{13}$  to  $1.08 \times 10^{13}$  molecules  $\text{cm}^{-3}$  and are displayed in Figure 3a. The experimental data were collected with varied ozone concentrations in mixing bulb 1 from  $1.81 \times 10^{14}$  to  $1.35 \times 10^{15}$  molecules  $\text{cm}^{-3}$  and are shown in Figure 3b. The experimental data were collected with varied  $\text{NO}_2$  concentrations in mixing bulb 1 from  $2.62 \times 10^{15}$  to  $2.24 \times 10^{16}$  molecules  $\text{cm}^{-3}$  and are displayed in Figure 3c. The experimental curve of condensation nuclei concentrations vs water vapor concentrations is displayed in Figure 3d.

### Discussion

The homogeneous gas-phase reaction of  $\text{NO}_2$  with ozone has been reported by a number of investigators.<sup>24-35</sup> The production of the  $\text{NO}_3$  and  $\text{N}_2\text{O}_5$  is described by the following chemical mechanism represented by the reactions below along with their measured rate constants at 298 K.



The reaction  $\text{NO}_2 + \text{O}_3 \rightarrow \text{NO} + 2\text{O}_2$  accounts for only ~3% of the  $\text{O}_3$ - $\text{NO}_2$  reaction and thus are not included in the list above. It is assumed that  $\text{O}_2$  and  $\text{N}_2$  have the same third-body efficiencies. The reaction of  $\text{NO}_2$  with  $\text{NO}_3$  can also yield the products  $\text{NO}$

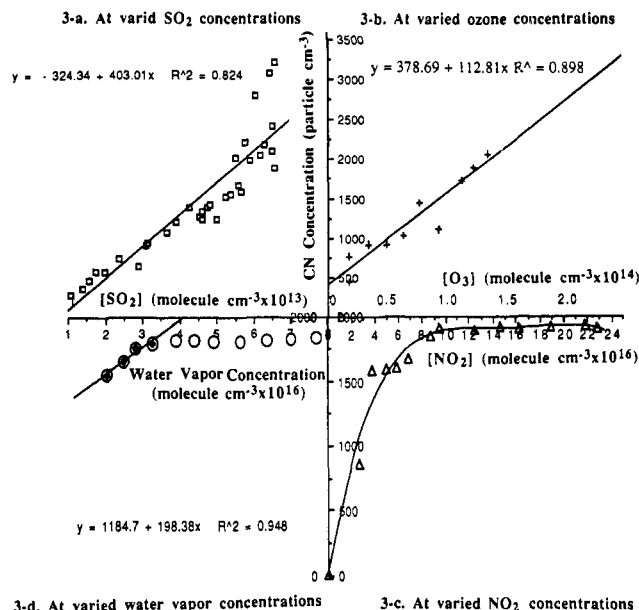


Figure 3. CN results at varying (a)  $\text{SO}_2$  concentrations; (b) ozone concentrations; (c)  $\text{NO}_2$  concentrations; and (d) water vapor concentrations.

+  $\text{NO}_2 + \text{O}_2$  (3). Since  $k_3 = 4.0 \times 10^{-16} \text{ cm}^3 \text{ molecule}^{-1} \text{ s}^{-1}$ , this reaction is approximately 4 orders of magnitude slower than that giving  $\text{N}_2\text{O}_5$ , (2), and hence is relatively unimportant. Therefore, the rate law for the production of  $\text{NO}_3$  and  $\text{N}_2\text{O}_5$  is as follows:

$$d[\text{NO}_3]/dt = k_1[\text{NO}_2][\text{O}_3] - k_2[\text{NO}_2][\text{NO}_3] + k_{-2}[\text{N}_2\text{O}_5] \quad (I)$$

$$[\text{N}_2\text{O}_5] = [\text{O}_3]_0 - [\text{O}_3]_t - [\text{NO}_3] \quad (II)$$

The rate law for the loss of  $\text{O}_3$  is  $-d[\text{O}_3]/dt = K_1[\text{NO}_2][\text{O}_3]$ . The integrated result is

$$[\text{O}_3]_t = [\text{O}_3]_0 / \exp(K_1[\text{NO}_2]_t t) \quad (III)$$

Substituting eqs II and III in eq I

$$d[\text{NO}_3]/dt = K_{-2}[\text{O}_3]_0 + [\text{O}_3]_t (K_1[\text{NO}_2]_t - K_{-2}) - [\text{NO}_3]_t (K_2[\text{NO}_2]_t - K_{-2})$$

Integration yields

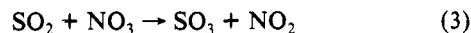
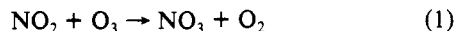
$$[\text{NO}_3] = (K_{-2}[\text{O}_3]_0 / (K_2[\text{NO}_2]_0 - K_{-2})) + ([\text{O}_3]_0 (K_1[\text{NO}_2]_0 - K_{-2}) / (K_2[\text{NO}_2]_0 - K_{-2} - K_1[\text{NO}_2]_0)) \exp(-K_1[\text{NO}_2]_0 t) + ([\text{O}_3]_0 (K_1[\text{NO}_2]_0 - K_{-2}) / (K_1[\text{NO}_2]_0 - K_2[\text{NO}_2]_0 + K_{-2}) - (K_{-2}[\text{O}_3]_0 / (K_2[\text{NO}_2]_0 - K_{-2}))) \exp(-(K_2[\text{NO}_2]_0 - K_{-2})t) \quad (IV)$$

Substituting eq IV in eq II gives

$$[\text{N}_2\text{O}_5] = [\text{O}_3]_0 - [\text{O}_3]_0 / \exp(K_1[\text{NO}_2]_0 t) - [(K_{-2}[\text{O}_3]_0 / [\text{O}_3]_0 (K_1[\text{NO}_2]_0 - K_{-2})) + [\text{O}_3]_0 (K_1[\text{NO}_2]_0 - K_{-2}) / (K_2[\text{NO}_2]_0 - K_{-2} - K_1[\text{NO}_2]_0)] \exp(-K_1[\text{NO}_2]_0 t) + ([\text{O}_3]_0 (K_1[\text{NO}_2]_0 - K_{-2}) / (K_1[\text{NO}_2]_0 - K_2[\text{NO}_2]_0 + K_{-2}) - (K_{-2}[\text{O}_3]_0 / (K_2[\text{NO}_2]_0 - K_{-2}))) \exp(-(K_2[\text{NO}_2]_0 - K_{-2})t) \quad (V)$$

For all conditions of operating the reactor, the relationships among the nitrogen oxide species were determined by the equilibrium represented by reactions 2 and -2, the value of the equilibrium constant being  $K_{\text{eq}} = k_2/k_{-2} = 2.2 \times 10^{-11} \text{ cm}^3 \text{ molecule}^{-1}$ . The mass balance of  $\text{NO}_3$  and  $\text{N}_2\text{O}_5$  was governed by the  $\text{O}_3$  concentrations, since reaction 1 ensured that the large excess of  $\text{NO}_2$  consumed almost all of the  $\text{O}_3$  in the time,  $t_1 = 45 \text{ s}$  before introduction into the reactor. Furthermore, the equilibrium relationship was maintained upon dilution by a factor of 110/1500 upon entering the reaction zone. All of these considerations are inherent in eqs IV and V which simplify greatly for most of the conditions of the experiments.

The time spent by the mixed reactants in the reactor,  $t_2$ , was 30.0 s in all of the experiments. The following reactions are considered to be those that could have occurred:



This analysis is to provide values of the rate constants  $k_3$  and  $k_4$  for the two reactions representing the oxidation of  $\text{SO}_2$ . First, it is necessary to calculate the concentrations of  $\text{NO}_3$  and  $\text{N}_2\text{O}_5$  in the reactor based on the known rate constants for reactions 1, 2, and -2, the upper limit for reaction 6, and experimental conditions. This will be shown below.

Application of eqs IV and V for experimental conditions in the reactor shows that, in the absence of removal by  $\text{SO}_2$  reactions, the concentrations of  $\text{NO}_3$  and  $\text{N}_2\text{O}_5$  remain constant during the 30-s traversal time in the reactor. This verifies that the equilibrium controls their relationships to each other and  $\text{NO}_2$ . For experiments in which  $[\text{NO}_2] = 2.27 \times 10^{16}$  molecules  $\text{cm}^{-3}$  and  $[\text{O}_3]_0 = 1.35 \times 10^{15}$  molecules  $\text{cm}^{-3}$  in mixing bulb 1, the resulting concentrations in the reaction zone are calculated to be  $[\text{NO}_3] = 2.08 \times 10^9$  molecules  $\text{cm}^{-3}$ ,  $[\text{N}_2\text{O}_5] = 9.92 \times 10^{13}$  molecules  $\text{cm}^{-3}$ .

The removal of  $\text{NO}_3$  and  $\text{N}_2\text{O}_5$  through reactions 3 and 4 is now estimated. The maximum concentration of  $\text{SO}_3$  can be calculated from the experimental data in which the maximum CN concentration was observed. By using the isomerization equation<sup>22</sup>  $[\text{CN}]/t = K_f[\text{SO}_3]$ ; and placing  $K_f = 4.0 \times 10^{-5} \text{ s}^{-1}$ ;  $[\text{CN}]_{\text{max}} = 3220$  (particle/ $\text{cm}^3$ );  $t = 30.0$  s, thus,  $[\text{SO}_3]_{t=30\text{s}} = 2.68 \times 10^6$  molecules  $\text{cm}^{-3}$ . It can be readily seen that this concentration is very small relative to those of  $\text{NO}_3$  and  $\text{N}_2\text{O}_5$  as indicated above. Therefore, these oxides of nitrogen were not significantly consumed by reactions with  $\text{SO}_2$ , and their equilibrium relationship is not perturbed.

It remains to evaluate the effectiveness of reaction 6 in removing  $\text{N}_2\text{O}_5$  in the reactor. The reaction,  $\text{N}_2\text{O}_5 + \text{H}_2\text{O} + \text{M} \rightarrow 2\text{HNO}_3 + \text{M}$ , has only a known upper limit for the rate constant,  $k_6 \leq 1.3 \times 10^{-21} \text{ cm}^3 \text{ molecule}^{-1} \text{ s}^{-1}$ . If the value of the upper limit is used, then a maximum removal of  $\text{N}_2\text{O}_5$  by this reaction during 30.0 s can be estimated by the expression:  $-d[\text{N}_2\text{O}_5]/dt = K_6[\text{N}_2\text{O}_5][\text{H}_2\text{O}]$ . Integration yields  $[\text{N}_2\text{O}_5]_0/[\text{N}_2\text{O}_5]_t = \exp(K_6[\text{H}_2\text{O}]t)$ . With  $[\text{H}_2\text{O}] = 7.68 \times 10^{16}$  molecules  $\text{cm}^{-3}$  and  $t = 30.0$  s,  $[\text{N}_2\text{O}_5]_0/[\text{N}_2\text{O}_5]_t = 1.003$ . This result indicates that reaction 6 does not significantly perturb the equilibrium of the oxides of nitrogen by rapidly removing  $\text{N}_2\text{O}_5$ . In addition, the wall reactions removing  $\text{N}_2\text{O}_5$  are eliminated by using the technique of uniform annular sheath flow.<sup>50</sup>

All of the calculations in this section thus show that the concentrations of  $\text{NO}_2$ ,  $\text{NO}_3$ , and  $\text{N}_2\text{O}_5$  are governed by equilibrium and that they are not significantly affected by reactions with  $\text{SO}_2$  and  $\text{H}_2\text{O}$ .

The results show that, in the experiments in which  $\text{NO}_2$  concentrations varied, the concentrations of  $\text{N}_2\text{O}_5$  remained constant (because of the constant  $\text{O}_3$  concentrations) and the concentrations of  $\text{NO}_3$  varied inversely with  $\text{NO}_2$  concentrations because of the equilibrium. There is only one data point showing a deviation from constancy, and it is in the wrong direction for  $\text{NO}_3$  to be considering the cause of the variation. If  $\text{NO}_3$  did play a detectable

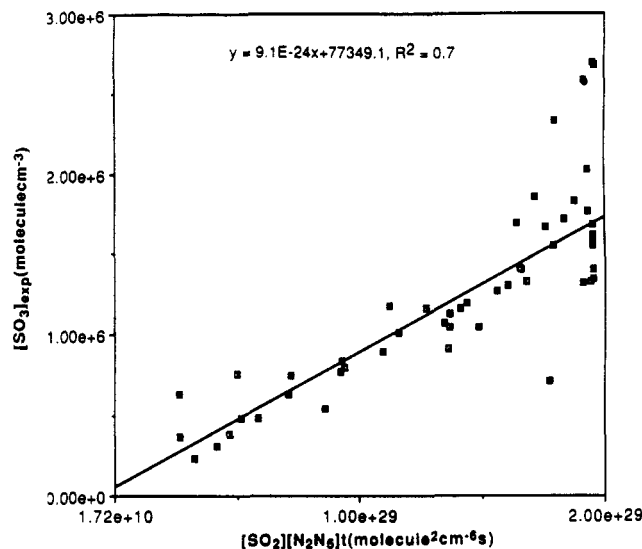


Figure 4. Linear regression analysis of  $[\text{SO}_3]_{\text{exp}}$  vs  $[\text{SO}_2][\text{N}_2\text{O}_5]$ . From the slope of the curve, the value of  $k_4$  is derived:  $k_4 = (9.1 \pm 0.38) \times 10^{-24} \text{ cm}^3 \text{ molecule}^{-1} \text{ s}^{-1}$ .

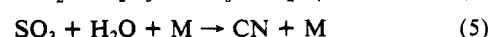
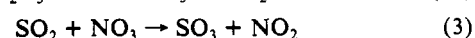
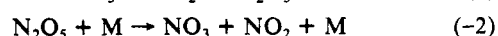
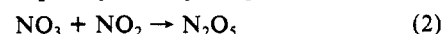
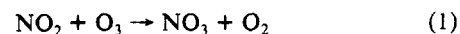
role, it would certainly have resulted in higher CN counts for lower  $\text{NO}_2$  concentrations.

The above discussion of the lack of an observable role for  $\text{NO}_3$  leaves as a reasonable conclusion that  $\text{N}_2\text{O}_5$  is the principal oxidant of  $\text{SO}_2$  in our experiments. The kinetic model for nuclei formation thus reduces to:  $\text{N}_2\text{O}_5 + \text{SO}_2 \rightarrow \text{SO}_3 + 2\text{NO}_2$  with the relationship of  $\text{NO}_2$  and  $\text{N}_2\text{O}_5$  controlled by the amount of  $\text{O}_3$ . The equilibrium among the oxides of nitrogen lies so far toward  $\text{N}_2\text{O}_5$  that the oxidation of  $\text{NO}_2$  by  $\text{O}_3$  can be considered to be stoichiometric. Thus, in all of the experiments  $[\text{N}_2\text{O}_5]_{\text{reactor}} = [\text{O}_3]_1/D$ , where 1 indicates the concentration in mixing bulb 1 and  $D$  is the dilution factor in the reactor. The kinetic rate expression is then  $d[\text{SO}_3]/dt = k_4[\text{SO}_2][\text{N}_2\text{O}_5]$  which, with the recognition that  $[\text{N}_2\text{O}_5]$  and  $[\text{SO}_2]$  remain constant in the reactor, gives  $[\text{SO}_3] = k_4[\text{SO}_2]([\text{O}_3]_1/D)t$ . In the analysis of data, the rate constant  $k_4$  is determined as the mean value found when  $[\text{SO}_3]_{\text{exp}}$  values are used in the relationship. The statistical analysis shows that  $k_4 = (9.1 \pm 0.38) \times 10^{-24} \text{ cm}^3 \text{ molecule}^{-1} \text{ s}^{-1}$  for the 56 experiments, which is performed in Figure 4. The error term is the standard error of the mean of the values of  $k_4$  calculated from the individual experiments.

To analyze the upper limit of the value of  $k_3$ , consider that in the set of experiments with varying  $\text{NO}_2$ , the highest  $\text{NO}_3$  concentration should have resulted at least in an increase of  $[\text{SO}_3]$  greater than the ratio of the standard deviation of  $k_4$  to the mean of  $k_4$  for that set of experiments. An analysis similar to that above for the calculation of  $k_4$  in terms of experimental concentrations leads to  $k_3 \leq 4.5 \times 10^{-21} \text{ cm}^3 \text{ molecule}^{-1} \text{ s}^{-1}$ .

## Conclusion

Experiments were performed to study reactions of  $\text{SO}_2$  with  $\text{NO}_3$  and  $\text{N}_2\text{O}_5$  to produce condensation nuclei. The production of condensation nuclei (CN) was observed under conditions in which the  $\text{NO}_2$  concentrations were in great excess of  $\text{O}_3$  concentrations. Analysis of the CN data recorded for sets of experiments in which  $\text{SO}_2$ ,  $\text{O}_3$ , and  $\text{NO}_2$  were systematically varied one at a time led to a deduced mechanism for the formation of the condensation nuclei and evaluation of the two rate constants  $k_3$  and  $k_4$ :



(50) Xie, Z. D. Condensation Nuclei Formation in the System of  $\text{SO}_2$ - $\text{N}_2\text{O}_5$  and in the Presence of Water Vapor. Doctoral Dissertation, Drexel University, 1991.

in which  $k_1 = 3.2 \times 10^{-17} \text{ cm}^3 \text{ molecule}^{-1} \text{ s}^{-1}$ ,  $k_2 = 1.3 \times 10^{-13} \text{ cm}^3 \text{ molecule}^{-1} \text{ s}^{-1}$ ,  $k_{-2} = 5.9 \times 10^{-2} \text{ cm}^3 \text{ molecule}^{-1} \text{ s}^{-1}$ ,  $k_3 \leq 4.5 \times 10^{-21} \text{ cm}^3 \text{ molecule}^{-1} \text{ s}^{-1}$ , and  $k_4 = 9.1 \times 10^{-24} \text{ cm}^3 \text{ molecule}^{-1} \text{ s}^{-1}$ .

A value of  $k_4$  has not been previously determined except as an upper limit ( $\leq 4.1 \times 10^{-23} \text{ cm}^3 \text{ molecule}^{-1} \text{ s}^{-1}$ ) by Daubendiek and Calvert,<sup>15</sup> with which the value found in this work is consistent.

Daubendiek and Calvert also found an upper limit for  $k_3$  of  $7.0 \times 10^{-21} \text{ cm}^3 \text{ molecule}^{-1} \text{ s}^{-1}$ . The present work provides a new, lower value of this upper limit.

*Acknowledgment.* The author wishes to thank Edward L. Doheny, Carl A. Silver, James P. Friend, Donald J. Perkey, and J. William A. Burley for their review of this work.

## FEATURE ARTICLE

### New Methods for Studying the Optical Properties of Metal Ions in Solids

Stuart M. Jacobsen, Brian M. Tissue, and William M. Yen\*

*Department of Physics and Astronomy, University of Georgia, Athens, Georgia 30602 (Received: July 8, 1991; In Final Form: September 18, 1991)*

We discuss recent advances in the synthesis and study of metal-ion-activated insulators. These materials are of interest in the development of tunable solid-state lasers. We focus our attention first on the synthesis of new materials in single-crystal fiber form, which is achieved by the laser-heated pedestal growth technique. Second, we discuss high-resolution optical techniques which have been developed to study these new materials, with emphasis on laser spectroscopy and fluorescence line narrowing in the near-infrared region. Finally, we summarize some of the latest trends and developments in the search for new transition-metal ions that will exhibit laser action in suitable host materials.

#### 1. Introduction

The optical properties of metal-ion-doped insulators have been the subject of many reports over the past decades by both physicists and chemists. One driving force behind the rapid growth of this field is the role played by these materials in the development of solid-state lasers.<sup>1</sup> For a comprehensive discussion on the subject of rare-earth-ion and transition-metal-ion optical centers, the reader is referred to various recent reviews and monographs.<sup>2</sup> In this article we will summarize some of the latest trends and developments in the synthesis and characterization of metal-ion-doped insulators. We will focus our attention on two relatively new techniques which have allowed us to take significant steps forward in our objectives of finding novel materials with desirable optical properties and of understanding the subtle static and dynamic properties of such materials. The first of these techniques involves the use of a high-powered laser beam to fabricate material in the form of single-crystal fibers. The second set of techniques are high-resolution laser spectroscopic methods for characterizing the materials.

We are particularly interested in obtaining crystalline oxides and fluorides doped or activated with a small amount of transition-metal-ion or rare-earth-ion impurity. Sometimes two different ions can be introduced together (codoping), and the possible interactions between them can be studied or can be utilized in the action of some optical device. The nature of the chosen host material essentially determines the geometry in which the active ion will find itself, which, in turn, determines the ordering and distribution of the activator's electronic energy levels. The host will also determine the vibrational modes around the dopant ion,

which will strongly influence the degree of nonradiative decay from the activator's excited states. The oxidation state of the impurity ion depends on the nature of the host crystal, as well as external parameters such as the presence of codopants and the atmosphere of the growth chamber. From the preceding discussion, therefore, it is clear that many factors are involved in the final specific properties of doped single-crystal insulators. For this reason it is highly desirable for the researcher to have at his disposal a fast, cost effective, and convenient means of growing crystals and thereby being able to quickly optimize all of the aforementioned parameters. In this way, the laser-heated pedestal growth (LHPG) of single-crystal fibers has literally revolutionized the way in which research in the optical properties of solids is conducted. The LHPG technique will be described in detail in section 2. As well as providing access to single crystals quickly and easily, the fiber geometry itself is advantageous in many respects.<sup>3</sup> One of these is the intriguing possibility of manufacturing miniature solid-state lasers, the waveguiding properties of the fiber enabling high-power densities to be reached within, thus lowering threshold for lasing and allowing modest pump powers which could be achieved with semiconductor diodes. Some of the existing tunable solid-state lasers are listed in Figure 1, along with the wavelength range in which they operate.

In section 3 we will discuss the spectroscopic techniques used in studying the optical properties of doped crystals. We will concentrate on the technique of fluorescence line narrowing (FLN) and, through examples in the recent literature, illustrate the unique information that it can make available.

#### 2. Laser-Heated Pedestal Growth

**Crystal Growth.** The LHPG method for pulling crystalline fibers has developed into an extremely powerful research tool,

(1) Budgor, A. B.; Esterowitz, L.; DeShazer, L. G. *Tunable Solid State Lasers II*; Springer-Verlag: Berlin, 1986.

(2) Henderson, B.; Imbusch, G. F. *Optical Spectroscopy of Inorganic Solids*; Oxford University: New York, 1988. Yen, W. M.; Selzer, P. M. *Laser Spectroscopy of Solids*; Springer-Verlag: Berlin, 1986. Yen, W. M. *Laser Spectroscopy of Solids II*; Springer-Verlag: Berlin, 1989.

(3) Yen, W. M. *Third Int. Conf. Trends Quantum Electron. 1988, SPIE 1033*, 183.